

International Journal of Mining and Mineral Engineering

ISSN online: 1754-8918 - ISSN print: 1754-890X

<https://www.inderscience.com/ijmme>

Active sensing in froth flotation

Mikko Salo, Teijo Juntunen, Risto Ritala

DOI: [10.1504/IJMME.2024.10063891](https://doi.org/10.1504/IJMME.2024.10063891)

Article History:

Received:	13 March 2023
Last revised:	30 August 2023
Accepted:	11 September 2023
Published online:	19 July 2024

Active sensing in froth flotation

Mikko Salo*, Teijo Juntunen and Risto Ritala

Department of Automation Technology and Mechanical Engineering,
Tampere University,
Tampere, Finland

Email: mikko.salo@tuni.fi

Email: teijo.juntunen@tuni.fi

Email: risto.ritala@tuni.fi

*Corresponding author

Abstract: The idea of active sensing is to embed sensor systems with intelligence to require less human interaction. Accurate but limited main measurement systems are complemented with broadband auxiliary measurements that gather data and alert the main measurement to focus on certain area. This is similar with the way that our eyesight works in context of gathering data from our surroundings. The purpose of this study is to introduce and test a control architecture that could improve the operation of froth flotation process. An active sensing architectures on linear quadratic Gaussian control is developed and tested in a simulation environment based on plant data for froth flotation with X-ray fluorescence and visible and near-infrared measurements. The architecture is tested in cases where external disturbances or auxiliary measurement model drifting go unnoticed by the main measurement. In both scenarios, the anomalies are successfully corrected by the active sensing architecture.

Keywords: active sensing; sensor management; linear-quadratic-Gaussian; LQG; froth flotation; Mahalanobis distance; POMDP.

Reference to this paper should be made as follows: Salo, M., Juntunen, T. and Ritala, R. (2024) 'Active sensing in froth flotation', *Int. J. Mining and Mineral Engineering*, Vol. 15, No. 2, pp.111–130.

Biographical notes: Mikko Salo holds MSc in Mathematics and in Automation Engineering. He has worked at the Tampere University's Faculty of Engineering and Natural Sciences in various projects since 2019. He is currently developing novel measurement technology for paper machines for his doctoral dissertation.

Teijo Juntunen obtained his MSc in Automation Engineering from Tampere University, Finland, in 2018. He is currently a doctoral researcher at the Tampere University's Faculty of Engineering and Natural Sciences, affiliated with the Research Unit of Automation Technaology and Mechanical Engineering. He specialises in data analysis and optimisation algorithms and is currently researching energy flexibility optimisation methodologies.

Risto Ritala holds a PhD in Technical Physics at Aalto University since 1986. After working in private sector till 2002, he has been a Professor in Measurement Information Technology at the Tampere University, retired since 2021.

1 Introduction

When concentrating minerals with the froth flotation process as the separation method, conventionally the X-ray fluorescence (XRF) analysers measure the concentrations online accurately but at a slow sampling rate, typically one measurement per five minutes. As XRF analysers are expensive, they commonly measure multiple slurry lines sequentially. As an alternative, spectral measurements that cover the visible and near-infrared (VNIR) ranges (400–1,000 nm) have been studied (Haavisto, 2009). These measurements have a high sampling rate (one measurement every 3 s) and are less expensive than XRF analysers. However, VNIR measurement is not as accurate as XRF measurement and it must be continuously calibrated based on the XRF measurement results. Some previous attempts at the control of the froth flotation process are reviewed in Quintanilla et al. (2021). Our study builds on this by developing a model predictive controller (linear-quadratic Gaussian) with exception handling. The used research methods are: system model identification using data from a commercial simulator of the froth flotation process, linear quadratic Gaussian controller tuning, and simulations of the process using the derived control and exception handling architecture in MATLAB environment.

As the XRF measurements are slow, their measurement schedule must be optimised. The deployment of XRF measurements in the use case of this paper is an example of the sensor management problem, defined as “control of the degrees of freedom in an agile sensor system to satisfy operational constraints and achieve operational objectives” (Hero and Cochran, 2011). The operational constraint here is the limited amount of measurement systems available and the operational objective is to obtain the best estimate of the process variables, which in the case of linear-quadratic-Gaussian (LQG) systems optimises also the control performance (Meier et al., 1967). Sensor management problems in process industry applications have been previously studied in, for example in Raunio and Ritala (2018). The sensor management problem is an example of a partially observable Markov decision process or POMDP (Sigaud and Buffet, 2013).

A control method based on LQG-control and exception handling is derived in this paper and tested in a simulated froth flotation process. We enhance the performance of the flotation line by optimising the sampling schedule of concentration measurement and analysing how an accurate sampling measurement is to be combined with a less accurate measurement that can measure concentrations at all sampling lines simultaneously. In particular, the latter measurement provides alarms to the former one about process upsets that the measuring schedule has prevented from observing directly. Should such an upset be severe enough, the normal schedule can be interrupted and the upset verified. The method derived in this paper is generalised for any similar process.

This paper is organised as follows. The froth flotation process, and XRF and VNIR measurements are shortly described in Section 2. In Section 3, the active sensing methods used in this study are defined: LQG control for determining the optimal measurement sequence with interruptions due to exceptional VNIR data. In Section 4 the architecture for general active sensing approach derived in this paper is explained. Section 5 defines the process model and ties the methods and algorithms introduced in Sections 3 and 4 for the use case of froth flotation. Section 6 reviews the simulation study results for the use case. Conclusions and discussion are presented in Section 7.

2 Process

2.1 Froth flotation

Froth flotation is the separation of minerals from each other according to the differences in the hydrophobicity of particles (Fuerstenau et al., 2007). A slurry of mixed minerals and water, the feed, enters a set of flotation tanks arranged in series, the flotation line. Each tank contains water, and a reagent is added to change the hydrophobicity of certain particles in the incoming slurry. Air is blown to the bottom of the tanks, making bubbles that encase the more hydrophobic particles, while the less hydrophobic ones remain in the tanks and continue to flow to the next tank. The particles caught by the air bubbles rise to the top of the tank forming the froth zone and then overflow out of the tank. The froth overflow rate is called the froth speed. The overflown froth from each tank is collected and is called the concentrate. The slurry that is not collected in any of the tanks in frothing is called tailings and flows out of the last tank in the line. The concentrate and tailings may be used as feed in another flotation line, where the separation of minerals is continued with different reagents and objectives.

The objective of the flotation process is to maximise the concentration of the wanted mineral in the concentrate, and the recovery of the wanted mineral from the original feed. The grade of the feed, concentrate and tailings is defined as the mass fraction of the wanted mineral in the slurry when water is excluded. Recovery is the fraction of the wanted mineral that is collected from the feed to the concentrate. A steady state value of the recovery can be calculated from feed, concentrate and tailings grades. Let F , C , T be the total masses of the feed, concentrate and tailings respectively, then the nonlinear recovery (in percentages) is

$$r_{nl} = \frac{Cc_a}{Ff_a} = 100 \frac{c_a(f_a - t_a)}{f_a(c_a - t_a)}, \quad (1)$$

where c_a, f_a and t_a are the values of concentrate, feed and tailings grades respectively. Equation (1) follows from the fact that mass is preserved, hence for mass fractions it holds that

$$Ff_a = Cc_a + Tt_a \quad (2)$$

and for total mass (multiplied by t_a) that

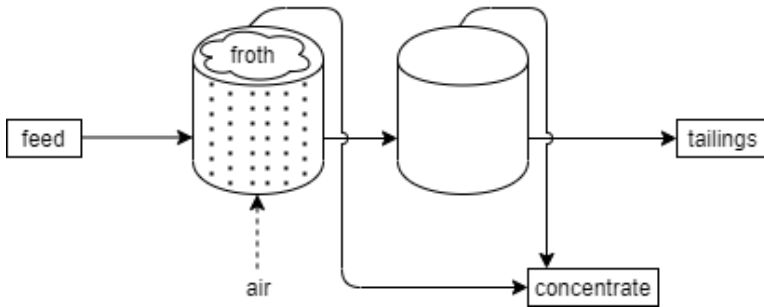
$$Ft_a = Ct_a + Tt_a. \quad (3)$$

Solving both for Tt_a and comparing yields

$$\frac{C}{F} = \frac{f_a - t_a}{c_a - t_a}$$

Both grade and recovery are controlled in a cascade by the froth speeds, which in turn are controlled mainly by the air flow into the tanks. A higher froth speed will yield a better recovery in the concentrate, but a lower grade. The control objective is to maintain the grade and recovery at a setpoint, chosen to be the appropriate balance between grade and recovery.

Figure 1 A diagram of the froth flotation process



2.2 XRF measurement

XRF technique is based on using excitation radiation on the sample to generate ionised atoms by photoelectric absorption. The fluorescence yield of these absorptions is measured with a spectrometer (Margui and Grieken, 2013).

In this study the main assay measurements were gathered from a plant with an XRF analyser. This analyser has a centralised structure where slurry samples are continuously fed to the analyser from different parts of the process through primary sampling pipes. A multiplexer then arranges the samples to be analysed sequentially from each primary line. Samples are analysed with a single X-ray tube and a spectrometer. A multivariate regression model to calculate assays from the measured spectra is calibrated with laboratory measurements (Haavisto, 2009).

Sample measurement time of an XRF analyser is typically 15–60 seconds in real applications and the number of measured streams varies between 6 to 18 depending on the type of the analyser. With these measurement times the accuracy of an XRF analyser under normal operation conditions is typically 3–6% relative standard deviation for minor concentrations and 1–4% for major concentrations when the mineral concentration levels are well above the minimum detection values of 0.001% of slurry weight.

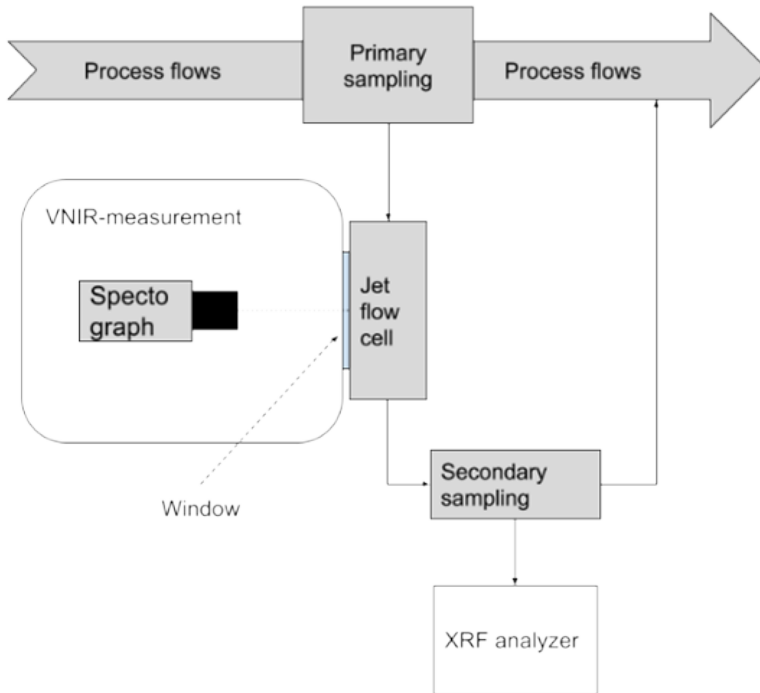
2.3 VNIR measurement

The colour of the froth in some mineral flotation processes correlates with the mineral composition in the froth (Gebhardt et al., 1993). Based on this correlation, there have

been studies on if the slow measurement rate of XRF-analysers can be improved on with reflective spectroscopy (Haavisto and Hyötyniemi, 2011).

In reflective spectroscopy the sample is first stimulated with electromagnetic radiation and then the intensity of the reflected light is measured. The wavelength range of VNIR is from the short wavelength visual, 400 nm to 2,500 nm where mid-wavelength infrared wavelength starts. However, in practical cases the VNIR range used covers wavelengths between 400 and 1,000 nm, because this is the most cost-effective range for measurement instruments.

Figure 2 VNIR and XRF measurements in the slurry line of the flotation process



In this study we have used the data collected from an industrial flotation process with both XRF- and VNIR-measurements as a basis for the simulated active sensing. Here VNIR-measurements were made every three seconds and the mean of last ten measurements is taken for concentration estimation with the latest model that has in turn been adapted according to the most recent XRF-measurement. Figure 2 shows the positioning of XRF and VNIR-measurements in the slurry line of the flotation process with respect to each other and the main process flow.

3 Optimal control with exception handling

3.1 LQG-control with active sensing

In this paper, LQG control is studied. The control action is based on an estimate of the current state of the process, and this estimate is based on measurements of the

process, making the measurement choices crucial for control efficiency. In unconstrained LQG problems, the optimal control law and measurement choice for each timestep have an exact solution that is separable with respect to control and measurement (Meier et al., 1967). Moreover, the measurement policy can be solved offline, with very little computations online required, given that the optimal sequence is applied without interruptions. However, in real processes optimal sequences must be occasionally interrupted due to for example external disturbances.

A process model is used to approximate the real process and to derive model predictive control. The model is a state space model linearised at the chosen operating point of the process. The process noise is assumed Gaussian, uncorrelated in time. The goal of the control is to minimise a cost function quadratic in deviations from the operating point. The process model is written as

$$x_{n+1} = Ax_n + Bu_n + \epsilon_n, \quad \epsilon_n \sim N(0, \Sigma^{(p)}) \quad (4)$$

The elements of the vector x_n are the states and elements of u_n are the control signals. The random vector ϵ_n is the process noise. It is normally distributed and has zero mean and the covariance matrix $\Sigma^{(p)}$ is diagonal, which means that the states are not correlated. The matrix A dictates how the states evolve in time with respect to each other. The matrix B dictates how the control signals affect the states. The measurement model of the process is

$$z_n = C_n x_n + \nu_n, \quad \nu_n \sim N(0, \Sigma_n^{(m)}) \quad (5)$$

where z_n is the measurement result. The matrix C_n is the measurement model matrix at time n . The measurement model at each time step is chosen amongst a set of values and number of rows according to the different measurement options of the process. The dimension of the measurement result z_n depends on the chosen measurement matrix and can be a scalar or a vector consisting of multiple measured outputs. The random vector ν_n is the measurement noise corresponding the chosen measurement model matrix C_n and has a diagonal covariance matrix $\Sigma_n^{(m)}$.

The real-life process state is represented by the Gaussian information state, which consists of an estimate of the state vector and uncertainty covariance matrix of the estimate. The information state is updated according to Kalman filter consisting the prediction step that updates the information state using the process model and the control action, and the measurement update step that updates the information state with measurement data.

We denote the estimate by μ_n and its uncertainty by Σ_n . The time index n is followed by a plus-sign if measurement data has been obtained in that time instance and Kalman filter measurement update has been made. A minus-sign following the time index notes that the measurement update has not yet been made at that time. With this notation, the Kalman filter prediction step updates the information state according to

$$\begin{aligned} \mu_{n+1-} &= A\mu_{n+} + Bu_n \\ \Sigma_{n+1-} &= A\Sigma_{n+}A^T + \Sigma^{(p)}. \end{aligned} \quad (6)$$

If a measurement result z_{n+1} is obtained from the real process, the Kalman filter update step updates the information state according to

$$L_{n+1} := \Sigma_{n+1-} C_{n+1} \left(C_{n+1} \Sigma_{n+1-} C_{n+1}^T + \Sigma_{n+1}^{(m)} \right)^{-1}$$

$$\begin{aligned}\mu_{n+1+} &= \mu_{n+1-} + L_{n+1}(z_{n+1} - C_{n+1}\mu_{n+1-}) \\ \Sigma_{n+1+} &= I - L_{n+1}C_{n+1}\Sigma_{n+1-}\end{aligned}\quad (7)$$

where C_{n+1} is the measurement model matrix corresponding the measured output results z_{n+1} and $\Sigma_n^{(m)}$ is the covariance matrix describing the corresponding measurement noise. The matrix I is an identity. The goal of the control is to minimise the expected value of a cost function quadratic in the measured outputs at each timestep n :

$$V_N[\mu_{n+}, \Sigma_{n+}] = \min \mathbb{E} \left(\sum_{i=0}^{N-1} (y_{n+i+1}^\top Q y_{n+i+1} + u_{n+i}^\top R u_{n+i}) \right) \quad (8)$$

where Q and R are symmetric positive-semidefinite matrices. These matrices define how much cost occurs when the system deviates from the operating point and when control action is taken. The vector $y_n = Cx_n$, where C is a matrix that is comprised of all the C_n stacked, are the measurable outputs of the state space model. Scalar N is the optimisation horizon. The minimisation is done by choosing control actions u_{n+i} and measurement options C_{n+i+1} up to the horizon N so that the cost function V_N attains its minimal value.

The cost function can be separated into two minimisations using the optimality of the Kalman filter and properties of random variables (Burl, 1999). One part is optimised solely over control actions and the other one solely over measurement actions. The cost function becomes

$$\begin{aligned}V_N[\mu_{n+}, \Sigma_{n+}] &= \min \left((u_n + K_N \mu_{n+})^\top \Phi_N (u_n + K_N \mu_{n+}) \right. \\ &\quad \left. + \mu_{n+}^\top Q_N \mu_{n+} \right) + \min_{\{C_{n+i}\}_{i=1}^{N-1}} \left(\text{tr}(Q \Sigma_{n+N-}) \right. \\ &\quad \left. + \sum_{i=1}^{N-1} \left(\text{tr}(Q \Sigma_{n+i-}) + \text{tr}(Q_{N-i} \Sigma_{n+i+}) \right) \right),\end{aligned}$$

where

$$\begin{aligned}\Phi_N &= R + B^\top(Q + Q_{N-1})B \\ K_N &= \Phi_N^{-1} B^\top(Q + Q_{N-1})A\end{aligned}$$

and Q_N is iterated as:

$$\begin{aligned}Q_N &= A^\top \left((Q + Q_{N-1}) \right. \\ &\quad \left. - (Q + Q_{N-1})B(R + B^\top(Q + Q_{N-1})B)^{-1}B^\top(Q + Q_{N-1}) \right) A \\ Q_0 &= 0.\end{aligned}$$

The minimisation with respect to control is solved by choosing $u_n = -K_N \mu_{n+}$ after finding Q_N Franklin et al. (2006). The minimisation with respect to measurement action sequence is a tree search: developing the estimate uncertainty up to the horizon N according to Kalman filter for each choice of measurement sequences $\{C_{n+i}\}_{i=1}^{N-1}$ and

then calculating the cost for each sequence and selecting the optimal cost (Meier et al., 1967). Pruning algorithms may be used to reduce the complexity of the calculations by not checking sub-optimal branches of the tree search (Ross et al., 2008).

At each timestep, the optimisation described above must be solved using the current estimate and its uncertainty. In the case of control, the estimate depends on the measurement data obtained, hence the control action cannot be computed offline. However, the factor K_N does not depend on time and thus the optimal control action is simple matrix multiplication given the current estimate. When optimising the measurement action, a tree search is necessary at each timestep and the first measurement is implemented to the real process. However, the estimate uncertainty is independent on measurement data; it depends only which measurement action has been chosen.

When the optimal measurement actions are taken the resulting uncertainties will converge to periodic sequence and thus the sequence of optimal actions is also periodic and can be solved offline. For this reason, an offline lookup-table of measurements may be formed using iterative optimisation until the measurements and uncertainties converge to a periodic sequence. This table may then be used when choosing the measurement actions assuming that the pattern is followed at all times.

Online calculations of the optimal measurement actions may be required to obtain optimal control upon starting the control when the information state is in transient phase, or when the measurement action sequence deviates at some time instant from the offline lookup-table for some reason. The offline lookup-table of optimal measurements is obtained with the following algorithm:

- 1 Set initial guess for state covariance matrix Σ_{n+}^0 .
- 2 Calculate optimal $\{C_{n+i}\}_{i=1}^{N-1}$ as described above starting from Σ_{n+}^0 .
- 3 Save C_{n+1} .
- 4 Set starting state covariance matrix Σ_{n+}^0 to Σ_{n+1+} resulting from Kalman filter and measurement C_{n+1} .
- 5 Repeat steps 2–4 until the saved measurements C_{n+1} in step 3 converge to a recurring pattern.
- 6 The recurring pattern is the optimal offline measurement sequence.

3.2 *Active sensing measurements*

The control architecture introduced in this paper has two distinct measurements: an accurate main measurement that measures only a subset of the outputs and an inaccurate auxiliary measurement that measures all outputs at the same time. The main measurement serves two purposes: the control of the process and updating the measurement model in the auxiliary system. The purpose of the auxiliary system is to alert the main system if it observes sudden deviation from the expected process behaviour, which is likely to be observed by the main system only with considerable delay. Sudden unexpected deviations in the outputs undetected by the main measurement may happen between the main measurements if the process time constants are

considerably smaller than the measurement interval, or in the periods when the main measurement system is measuring other outputs.

The Kalman filter update step is applied recursively for each different measurement result obtained at the same timestep. The information state updated by data from both the main and auxiliary measurement systems is referred to as the primary information state and the information state updated only by data from the main measurement system is referred to as secondary (similarly primary/secondary estimate and estimate uncertainty).

3.3 Exception handling

The main measurement and the auxiliary measurement must be compared with each other at each time step of the process in question. Since both measurements are usually executed at different times, it is necessary to estimate how well the latest measurement represents the current state of the process, i.e., at each time instant an estimate of the uncertainty for a measurement has to be known as a function of time that has passed since the latest measurement. This uncertainty also includes the inherent process and measurement noises. The surprise factor between main and auxiliary measurements can be estimated with Mahalanobis distance-based (Mahalanobis, 1930) number as follows.

The Mahalanobis distance D between the Gaussian main measurement information X_n^p and the Gaussian auxiliary measurement information X_n^s at the time instant n is

$$D_n = (\mu_{p,n} - \mu_{s,n})^T (\Sigma_{p,n} + \Sigma_{s,n})^{-1} (\mu_{p,n} - \mu_{s,n}) \quad (9)$$

where $\mu_{p,n}$ is the expected value of the process state based on the main measurement at time instant n , $\mu_{s,n}$ is the expected value of the process state based on the auxiliary measurement at same time instant, $\Sigma_{p,n}$ is the uncertainty covariance matrix of the main measurement information and $\Sigma_{s,n}$ is the uncertainty covariance matrix of the auxiliary measurement.

If the main measurement can be approximated to be exact, the covariance $\Sigma_{p,n}$ can be evaluated from process data using pure random walk model (Appendix A). If the main measurement cannot be approximated to be exact, the uncertainties must be estimated otherwise such as comparing the measurement data with other measurements known to be exact.

A probability $p(D_n)$ then indicates when the auxiliary measurement differs from the main measurement more than the amount of D_n .

$$\begin{aligned} P(D_n) &= \int_{(x-\mu)^T \Sigma^{-1} (x-\mu) > D} (2\pi)^{\frac{d}{2}} \exp\left(-\frac{1}{2}(x-\mu)^T \Sigma^{-1} (x-\mu)\right) d^d \\ &= \frac{\Gamma\left(\frac{d}{2}, \frac{D}{2}\right)}{\Gamma\left(\frac{d}{2}\right)} \end{aligned} \quad (10)$$

where d is the dimension of the state vector, $\Gamma(s)$ is the gamma function and $\Gamma(s, x)$ is the incomplete gamma function. The difference is statistically significant at level p when $p(D_n) < p$. For example, if there is a sudden change in the process but there has not been a main measurement after that change the Mahalanobis distance grows and the auxiliary estimate differs significantly from the main estimate.

4 Architecture for active sensing

The LQG-control and exception handling introduced in Section 3 together form an active sensing control architecture used to control the process optimally under normal conditions, as well as to detect and handle any issues arising from external disturbances or auxiliary measurement model errors.

Figure 3 Control and measurement architecture (see online version for colours)

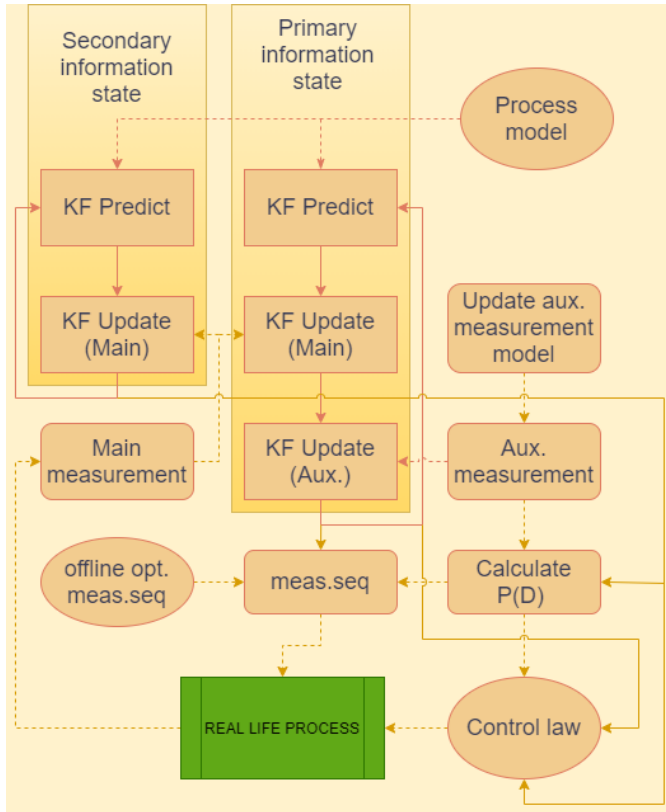


Figure 3 depicts the control and measurement architecture. At each time step:

- 1 Main measurement data is obtained from the real process.
- 2 Both information states are updated according to Kalman filter and the process model and main measurement data.
- 3 The auxiliary measurement model is updated according to measurements made by the main measurement system.
- 4 Auxiliary measurement data is calculated according to the auxiliary measurement model and measurement system signal from the process.
- 5 Primary information state is updated according to Kalman filter and auxiliary measurement data.

- 6 The $P(D)$ values are calculated for each output.
- 7 The next main measurement and control law are chosen accordingly and applied to the real process.

There are three distinct cases when choosing the next timestep main measurement and control action. Under normal operation, the main measurement and control action are chosen from the offline optimal measurement sequence according to LQG-control defined in Subsection 3.1. The operation is considered normal when the primary information state uncertainty is close to some state covariance matrix of the optimal offline measurement sequence in terms of matrix norm. Normal operating conditions also assume that no exceptions occur.

If exceptions have occurred, the next main measurement will be chosen according to the largest $P(D)$ value obtained according to Subsection 3.3, and the control law will use the secondary estimate in the case of the outputs that have experienced an exception. If no exceptions have occurred, but the information covariance is in transient rather than in the regular offline-optimised value, the next main measurement will be calculated online according to optimal LQG control.

The exceptions are detected by the auxiliary measurement. The auxiliary measurement model is updated and will drift and yield erroneous data if not updated. The auxiliary measurement result may deviate significantly from the secondary estimate because of two alternative reasons: there has been a sudden process upset or the measurement model of the secondary measurement has deteriorated considerably. To distinguish between the two potential causes, the periodic sampling sequence is interrupted, and the corresponding sampling line is measured with the main measurement. If the significant deviation is due to the process, the estimates are updated based on new main measurement data, whereas if it is due to deteriorated measurement model, the model is updated with the main measurement data.

5 Active sensing for flotation process

The combination of LQG control and exception handling developed was tested and demonstrated in a simulation of a single copper enrichment flotation line of eight flotation tanks. An eight tank-simulation (Kortelainen, 2019) in the Outotec HSC Chemistry 9 – simulator, hereby referred to as the process, was used to run step response tests and the data obtained was used to build a linear state space model of the process

5.1 System dynamics

The manipulatable inputs of the process are the setpoints of the froth speeds in tank groups 1–4 and tank groups 5–8. These are referred to as FrothSpeed1 and FrothSpeed2, respectively. The feed grade is considered as a measurable, but non-controllable load disturbance and it is modelled as a near-random walk. The controllable and measurable outputs of the process are the concentrate grade and the tailings grade. The model has 19 states whose linear combinations form the outputs and one state that represents the disturbance component. The inputs, disturbance and the outputs of the model represent deviations from a linearisation point rather than their actual values. The discretisation interval of the model is 300 seconds.

The state and control dynamics matrices as well as the measurement matrices of the model were identified with step response tests in the HSC-simulator. Step inputs in the controls and the disturbance were made separately and the outputs were recorded. The time was discretised to match the main measurement frequency. The discretisation interval is much smaller than the relevant time constants of the process. Linear state space models were fitted to match each discretised input-output data pair. The linear models were then combined into a multiple-input multiple-output state-space model. The dynamics and measurement matrices of the model are presented in Appendix B. The linearisation point values are depicted in Table 1.

Table 1 Linearisation point

f_0	0.91%
c_0	3.50%
t_0	0.047%

The process noise is set so that it appears as a zero mean gaussian white noise in the measurable outputs with a standard deviation of 10% (30% for feed grade) of the maximum perturbations in the step response tests. The covariance matrix of the process noise for the outputs is then

$$\Sigma^{(p,o)} = \begin{bmatrix} 0.0671 & 0 & 0 \\ 0 & 0.3179 & 0 \\ 0 & 0 & 0.0015 \end{bmatrix} * 10^{-3}.$$

This is converted to state process noise by finding a diagonal covariance matrix $\Sigma^{(p)}$ that minimises the residual norm

$$C\Sigma^{(p)}C^T - \Sigma^{p,o}. \quad (11)$$

In other words, the state process noise covariance matrix $\Sigma^{(p)}$ is set so that it produces a close approximation of the wanted noise with a covariance matrix $\Sigma^{(p,o)}$ in the outputs.

5.2 Measurement models

The model has two measurements: one representing the VNIR measurement, which is less accurate but can measure all the grades at each time instant. The VNIR measurement result is modelled with the matrix C . The vector $y_n = Cx_n = [f, c, t]^T$, where x_n are the states, represents deviations of the measurable outputs of the model from the linearisation point: feed grade (f), concentrate grade (c) and the tailings grade (t). The VNIR measurement result at time n is $z_{V,n} = Cx_n + v_{V,n}$, where $v_{V,n}$ is the VNIR measurement noise. The measurement noise depends on time, since the VNIR model is updated with the XRF measurement data and the accuracy of the VNIR model depends on the time since the most recent measurement with the XRF.

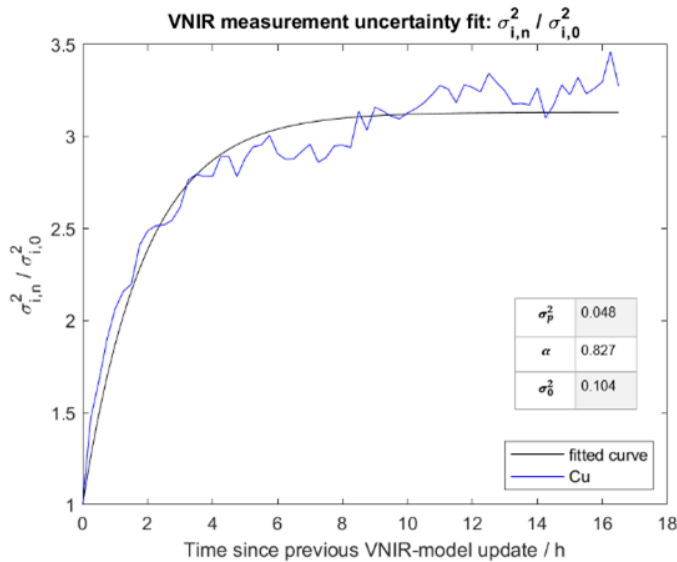
XRF measurement result at time n is $z_{C,n} = C_n x_n + v_{C,n}$, where C_n is a row of C depending on which output the XRF is measuring. The XRF measurement noise $v_{C,n}$ depends on which grade is measured and is proportional to the magnitude of the

measured quality. The standard deviation of the XRF measurement is set to $0.05f_0$, $0.03c_0$ and $0.08t_0$ for feed, concentrate and tailings grade measurements respectively.

The VNIR model is updated and VNIR measurements are made only whenever XRF measurement data is obtained in this use case. The XRF measurement interval is smaller than the relevant time constants of the process, so no significant changes happen between single discrete timesteps. The VNIR measurement acts to observe changes in the process in all outputs at the same time, when XRF can observe only one at a given time.

The VNIR measurement noise $\nu_{V,n}$ was calculated from six weeks of VNIR measurements collected from a flotation process plant. This data was then used to analyse how the uncertainty of VNIR-measurement increases as a function of time from the most recent model update. The models that convert the spectral data of VNIR measurements into concentration values are updated after every XRF measurement. To get a good sampling of update intervals, older models were also used to calculate concentrations from VNIR measurements.

Figure 4 VNIR measurement uncertainty for copper measurement as a function of time from previous update with fit parameters (see online version for colours)



The XRF measurement was considered to be exact for the purposes of evaluating the VNIR measurement uncertainties. Thus, the VNIR measurement error $d(t)$ is the difference between XRF and VNIR measurements. Here t is the time from the model update. The $d(t) : s$ were grouped into ten-minute sets so that t -window for each group was ten minutes long. The variance of each group representing the uncertainty of the VNIR measurement at that time since the last model update.

From the shape of the $d(t)$ curve in Figure 4 the model to be fitted to this data was decided to be of form:

$$\sigma_{i,n}^2 = \alpha^n \sigma_{i,0}^2 + \sigma_{i,p}^2 \frac{1 - \alpha^n}{1 - \alpha} \quad (12)$$

where $\sigma_{i,0}^2$ is the variance of concentration i when t is 0 and n is the update-interval in minutes. The fit parameters are α and $\sigma_{i,p}^2$, of which α denotes the transitional rate from minimum variance $\sigma_{i,0}^2$ to saturated variance $(\sigma_{i,p}^2)/(1 - \alpha)$. These fitted parameter values for each measured component can be seen in Figure 4.

This fit is then scaled in the linearisation point (f_0, c_0, t_0) of the system. Also, the VNIR measurement noise needed for each time step in exception handling is estimated from this fit. This method can also be applied to other process components if needed.

5.3 Control goal

The control actions are applied according to the optimal control law discussed in Section 3.1. The estimate used to calculate the control is chosen according to Section 4. The control goal is to minimise the LQG cost function (8). A linearised representation of the steady state concentrate recovery is added to the cost function as a controllable variable. The linearisation is done by a second order Taylor polynomial. The linearised concentrate recovery is

$$r = J_f f + J_c c + J_t t, \quad (13)$$

where J_i are the partial derivatives of nonlinear recovery (1) in the linearisation point and f , c , t are the model disturbance and outputs. The linearised concentrate recovery represents a deviation of the recovery from its linearisation point $r_0 = 96.13\%$. The cost function is of the form

$$V_N[\mu_{n+}, \Sigma_{n+}] = \min \mathbb{E} \left(\sum_{i=0}^{N-1} Q_c c_{n+i+1}^2 + Q_t t_{n+i+1}^2 + Q_r r_{n+i+1}^2 + u_{n+i}^\top R u_{n+i} \right), \quad (14)$$

where Q_i are the weighting parameters of the controllable variables and are set when tuning the control. This converts to the standard form LQG cost function with

$$Q = \begin{bmatrix} Q_r J_f^2 & Q_r J_f J_c & Q_r J_f J_t \\ Q_r J_f J_t & Q_c + Q_r J_c^2 & Q_r J_c J_t \\ Q_r J_f J_t & Q_r J_c J_t & Q_t + Q_r J_t^2 \end{bmatrix}$$

and the measurable output vector $y = [f, c, t]^\top$. The vector u consists of the controls and their weighting matrix R is set when tuning the control.

6 Simulation studies

6.1 Test environment

The simulations are run as a MATLAB script. The script consists of roughly three components: model definition, solving the optimal offline measurement sequence and control law, and the actual simulation.

The model is defined as the pre-determined state space model and parameters are set described in Subsection 5.1. In order to study different scenarios the LQG cost function weighting parameters are varied in simulations. The measurement sequence and control law are optimised offline according to Subsection 3.1. The simulation loops in time as described in Section 4.

6.2 Optimal measurement in normal operating conditions

The effect of LQG cost function weighting parameters to the optimal offline measurement sequence was tested. The weights were given a default value which are depicted in Table 2.

Table 2 Default output weighting parameters

$Q_{c,0}$	c_0^{-2}
$Q_{t,0}$	t_0^{-2}
$Q_{r,0}$	r_0^{-2}

The default weights are set so that in the linearisation point, all outputs are given equal weight in the cost function. These default weights were given different multipliers w_c , w_t , w_r ($Q_c = w_c Q_{c,0}$, etc.) and the resulting optimal offline measurement sequence was recorded. The results are depicted in Table 3. The measurements are indexed 1, 2, 3 for feed, concentrate and tailings grades respectively.

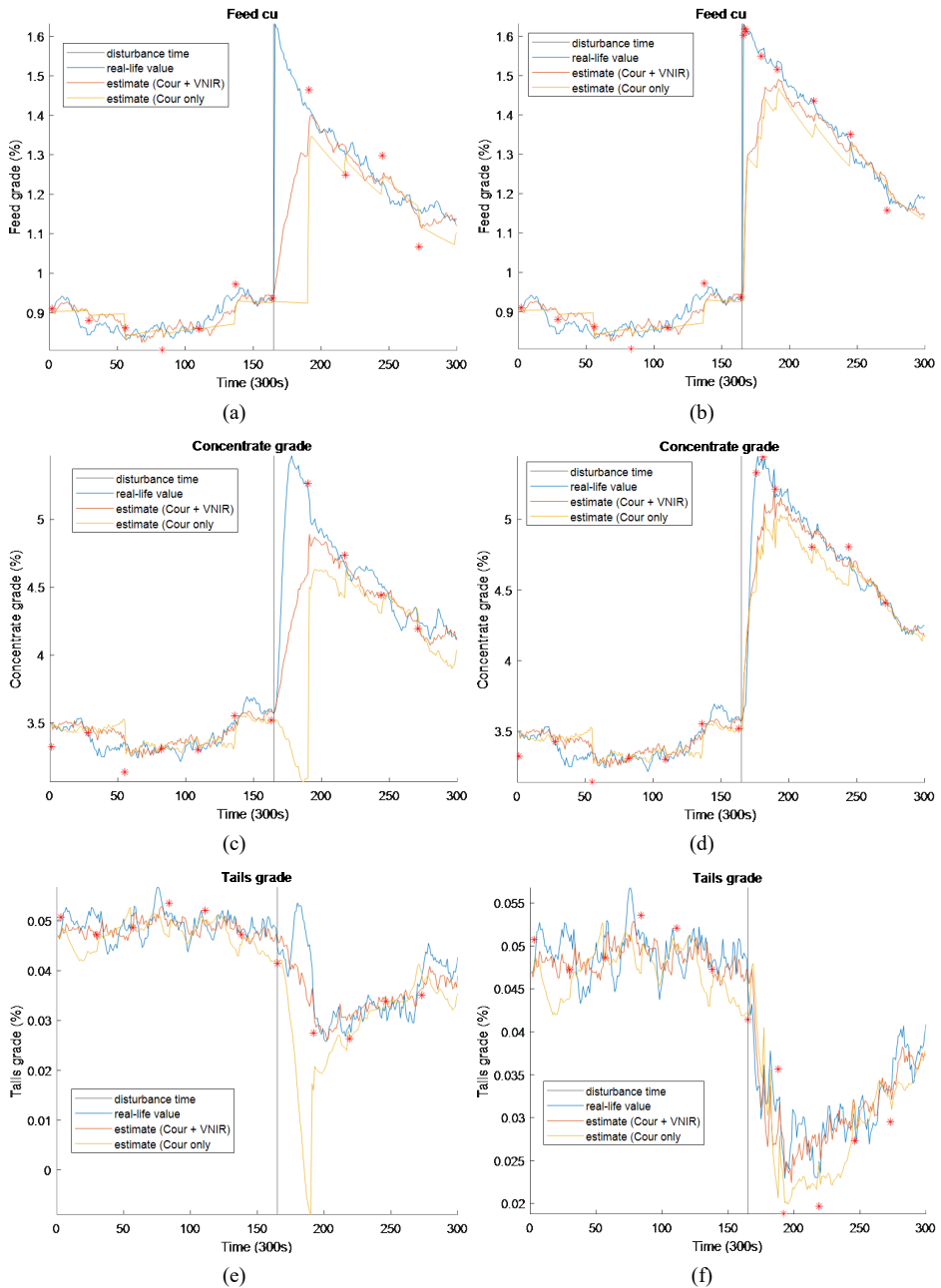
Table 3 Effect of choice of weighting parameters to optimal measurement sequence

$[w_c, w_t, w_r]$	Optimal offline measurement sequence
[1, 1, 1]	3-2-3-1
[2, 1, 1]	3-2-1
[150, 1, 1]	1-2-2-1-2
[1, 10, 1]	3-3-3-3-3-2
[1, 1, 30]	3-1-3-2-3-1

6.3 Exception handling in case of external disturbances

The ability of the exception handling to detect external disturbances when XRF measurements are very limited was tested. The XRF was assumed to measure each output of the modelled line equally. The measurement model was extended with a fourth measurement to simulate the XRF servicing other flotation lines. The XRF was set to measure the other flotation lines for 24 out of the 27 timesteps, with the remaining three servicing the modelled line. When the XRF is servicing other lines, the Kalman filter update step for the information state of the modelled line is an identity map, meaning only model prediction and VNIR update are used. The online measurement optimisation option was turned off since the other flotation lines are not modelled which would cause the online optimisation to trigger constantly.

Figure 5 Disturbance simulation results, (a) feed without exception handling (b) feed with exception handling (c) conc. without exception handling (d) conc. with exception handling (e) tails without exception handling (f) tails with exception handling (see online version for colours)



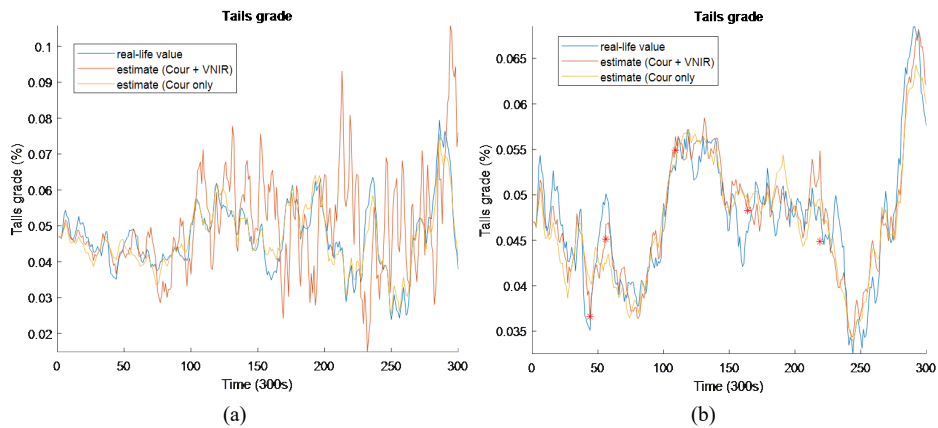
Note: Red stars depict XRF measurements.

A stepwise external disturbance of magnitude 0.7 was introduced to the feed grade right after XRF had just measured it, meaning the next measurement is scheduled to 27 timesteps away. The behaviour of the outputs and the estimates in cases where exception handling is turned on/off were recorded and are depicted in Figure 5.

6.4 Exception handling in case of VNIR model inaccuracy

In this test, the VNIR measurement model was assumed to drift if not calibrated regularly. Only the modelled flotation line was used, and the LQG cost function weighting parameters were chosen such that the XRF measurement will not measure tailings grade at all under normal operating conditions. The actual VNIR measurement noise was assumed to start drift after it has not been calibrated in 50 timesteps. The measurement noise variance was assumed to increase 1% for every timestep after 50 that the VNIR has not been calibrated for that output, while the model in the exception handling calculations was assumed to behave as in Subsection 5.2. The VNIR model was assumed to be corrected when the output is measured by the XRF.

Figure 6 VNIR model drift simulation results, (a) tails without exception handling (b) tails with exception handling (see online version for colours)



Note: Red stars are XRF measurement results.

The tailings grade and its estimates were recorded in cases where exception handling is turned on/off and are depicted in Figure 6.

7 Discussion and conclusions

The simulation test results show improvement when the derived architecture is used. In Subsection 6.2, the optimal measurement is shown to depend on the chosen goals of the control. When an output is given a larger weighting factor, the optimal offline measurement sequence will measure that output more frequently.

In Subsection 6.3, the process model is extended to consider multiple flotation lines. The exception handling detects an unpredicted process disturbance and alerts the

XRF measurement to verify it and correct the estimates. Significant improvement in the ability to estimate the real state of the process can be seen. Similar unpredicted disturbances could happen in all the flotation lines of a plant that has limited XRF-measurements available. This would mean that the XRF could be scheduled so that it follows an optimal pattern (in case that all the flotation lines can be modelled) with the exception handling enabled. A more realistic scenario that does not require a complicated model would be that the XRF measures all the outputs in some order with the exception handling enabled, alerting the XRF whenever it is needed. If alerts from different outputs would occur frequently, data of the alerts could be used to generate a measurement pattern.

In Subsection 6.4, the VNIR model was assumed to drift from the assumed model. The exception handling detects the model drift and alerts the XRF to calibrate it. The drifting model produces estimates useless for control. In case of multiple flotation lines, an optimal measurement sequence in terms of LQG-control could easily not contain one of the outputs at all since the model predictive control will deduce some outputs from the others easily. However, such a sequence will not take into account the drifting VNIR model, hence the exception handling is critical.

As in the case of any closed loop control, the LQG does not function well when the measurements are very limited and the operation of the process deviates from the given model. When the unknown process disturbances happen only in part of the process, the simulation studies show that the limited main measurement can be utilised to detect and correct them given that the disturbance can be detected. This is the case with the auxiliary measurement, that can not in itself be used for estimation and control due to its inaccuracy. Scheduling the limited main measurements with the auxiliary measurement data is shown to improve the quality of the estimates without human interaction, which is the goal of active sensing.

References

- Burl, J.B. (1999) *Linear Optimal Control: H_2 and H_∞ Methods*, Addison-Wesley, Menlo Park, CA.
- Franklin, G., Powell, J.D. and Workman, M.L. (2006) *Digital Control of Dynamic Systems*, 3rd ed., January, Addison-Wesley, Menlo Park, CA.
- Fuerstenau, M.C., Jameson, G.J. and Yoon, R.H. (2007) *Froth Flotation: A Century of Innovation*, Society for Mining, Metallurgy, and Exploration, Littleton, Colo.
- Gebhardt, J.E., Tolley, W.K. and Ahn, J.H. (1993) 'Color measurements of minerals and mineralized froths', *Mining, Metallurgy & Exploration*, Vol. 10, No. 2, pp.96–99.
- Haavisto, O. and Hyötyniemi, H. (2011) 'Reflectance spectroscopy in the analysis of mineral flotation slurries', *Journal of Process Control*, Vol. 21, No. 2, pp.246–253.
- Haavisto, O. (2009) *Reflectance Spectrum Analysis of Mineral Flotation Froths and Slurries*, Yliopistopaino, Helsinki.
- Hero, A.O. and Cochran, D. (2011) 'Sensor management: past, present, and future', *IEEE Sensors Journal*, Vol. 11, No. 12, pp.3064–3075.
- Kortelainen, J. (2019) *Utilization of Digital Twin in Model-Based Control of Flotation Cells*, Master's thesis, LUT School of Energy Systems, Finland.
- Mahalanobis, P.C. (1930) 'On tests and measures of group divergence', *Journal of the Asiatic Society of Bengal*, Vol. 26, No. 4, pp.541–588.
- Margui, E. and Grieken, R.v.R. (2013) *X-ray Fluorescence Spectrometry and Related Techniques: An Introduction*, Momentum Press, 222 East 46th Street, 10017, New York, NY.

- Meier, L., Peschon, J. and Dressler, R. (1967) ‘Optimal control of measurement subsystems’, *IEEE Transactions on Automatic Control*, Vol. 12, No. 5, pp.528–536.
- Quintanilla, P., Neethling, S.J. and Brito-Parada, P.R. (2021) ‘Modelling for froth flotation control: a review’, *Minerals Engineering*, Vol. 162, No. 3, p.106718.
- Raunio, J-P. and Ritala, R. (2018) ‘Active scanner control on paper machines’, *Journal of Process Control*, Vol. 72, No. 12, pp.74–90.
- Ross, S., Pineau, J., Paquet, S. and Chaib-Draa, B. (2008) ‘Online planning algorithms for POMDPS’, *The Journal of Artificial Intelligence Research*, Vol. 32, No. 2, pp.663–704.
- Sigaud, O. and Buffet, O. (2013) *Markov Decision Processes in Artificial Intelligence: MDPs, beyond MDPs and Applications*, March, Wiley-Blackwell, Hoboken, NJ.

Appendix A

Estimating the covariance matrix of an exact main measurement

The covariance matrix $\Sigma_{C,n}$ for each moment n can be evaluated from the gathered process data. When the process model is not known, a pure random walk model is used:

$$\begin{aligned} X_n &= X_{n-1} + E_n \\ E_n &\sim N\left(0, \Sigma^{(p)}\right) \end{aligned}$$

where timestep is one minute. It is assumed that a main measurement is executed at moment n and it is exact. It is also assumed that the next main measurement is executed at moment $n + N$ and it is also exact. Then

$$X_{n+N} = X_n + \sum_{i=1}^N E_{n+i}$$

Because the noise terms are independent, information about the state of the system before the measurement at time $n + N$, which is the measure-based estimate of said moment and its uncertainty, can be described by the distribution:

$$X_{n+N} \sim N\left(X_n, N \cdot \Sigma^{(p)}\right)$$

On the time instant $n + N$ a sample of this random variable is gained, which can then be used to estimate the process covariance matrix $\Sigma^{(p)}$. If the measurements were evenly spaced, it would hold that

$$(X_{n+N} - X_n) \sim N\left(0, N \cdot \Sigma^{(p)}\right)$$

so the covariance of the consecutive observations is the estimate $N \cdot \Sigma^{(p)}$. It also holds true that:

$$\left(\frac{X_{n+N} - X_n}{\sqrt{N}}\right) \sim \left(0, \Sigma^{(p)}\right)$$

which can be applied for unevenly spaced data. Let the measurements happen at time instants n_0, \dots, n_k , the algorithm for estimating the $\Sigma^{(p)}$ is:

